

2016

# Dissociative electron attachment to halogen molecules: Angular distributions and nonlocal effects

Ilya I. Fabrikant

*University of Nebraska-Lincoln*, ifabrikant@unl.edu

Follow this and additional works at: <http://digitalcommons.unl.edu/physicsfabrikant>

---

Fabrikant, Ilya I., "Dissociative electron attachment to halogen molecules: Angular distributions and nonlocal effects" (2016). *Ilya Fabrikant Publications*. 8.

<http://digitalcommons.unl.edu/physicsfabrikant/8>

This Article is brought to you for free and open access by the Research Papers in Physics and Astronomy at DigitalCommons@University of Nebraska - Lincoln. It has been accepted for inclusion in Ilya Fabrikant Publications by an authorized administrator of DigitalCommons@University of Nebraska - Lincoln.

**Dissociative electron attachment to halogen molecules: Angular distributions and nonlocal effects**

I. I. Fabrikant

*Department of Physics and Astronomy, University of Nebraska, Lincoln, Nebraska 68588-0299, USA*

(Received 23 August 2016; published 28 November 2016)

We study dissociative electron attachment (DEA) to the CIF and F<sub>2</sub> molecules. We formulate a method for calculation of partial resonance widths and calculate the angular distributions of the products in the CIF case using the local and nonlocal versions of the complex potential theory of DEA. They show the dominance of the *p* wave except in a narrow energy region close to zero energy. Comparison of the local and nonlocal DEA cross sections show that the former are smaller than the latter by a factor of 2 in the energy region important for calculation of thermal rate coefficients. This result is confirmed by comparison of the local and nonlocal calculations for F<sub>2</sub>. Only at low energies below 30 meV the local cross sections exceed nonlocal due to the 1/*E* divergence of the local results. On the other hand, the thermal rate coefficients generated from the local cross sections agree better with experiment than those calculated from the nonlocal cross sections. The most likely reason for this disagreement is the overestimated resonance width in the region of internuclear distances close to the point of crossing between the neutral and anion potential-energy curves.

DOI: [10.1103/PhysRevA.94.052707](https://doi.org/10.1103/PhysRevA.94.052707)**I. INTRODUCTION**

Comparative studies of dissociative electron attachment (DEA) to halogen molecules is interesting for several reasons. Due to high electron affinity of halogen atoms these reactions are exothermic and occur with relatively high rates. Low-energy DEA to homonuclear halogen molecules, like F<sub>2</sub> and Cl<sub>2</sub>, is dominated by the Σ<sub>u</sub> resonance with the *p* wave as a main component [1,2]. This leads, according to the Wigner threshold law for exothermic reactions [3], to *E*<sup>1/2</sup> behavior of the cross section as a function of electron energy *E* at low values of *E*. Confirmation of this prediction became possible after development of laser electron attachment method [4] generating very highly resolved in energy electron beams. The Wigner threshold law was observed for Cl<sub>2</sub> [5,6] and F<sub>2</sub> [7]. Another confirmation was obtained by comparison of calculated and measured thermal rate coefficients for these halogen compounds [8,9]. The theoretical calculations were carried out within the framework of the nonlocal complex potential theory [10] and equivalent resonance *R*-matrix theory [11]. This is essential for the threshold behavior since the local theory generates cross sections diverging as 1/*E* at *E* → 0.

There are no systematic studies of local versus nonlocal dynamics for DEA processes. It is known that the local theory for DEA fails in the case of a broad shape resonance with a typical example of low-energy DEA to the H<sub>2</sub> molecule [10,12] driven by a very broad <sup>2</sup>Σ<sub>u</sub> resonance. A similar situation is observed in the case of hydrogen halides [13–15] where, in addition to the effect of the broad resonance, the long-range dipolar interaction strongly affects the DEA dynamics which cannot be described by the local theory. On the other hand, in the case of a relatively narrow resonance at not very low energies and in the absence of a strong long-range interaction, the local theory was demonstrated to be very successful. Typical examples are CF<sub>3</sub>Cl molecule [16] and acetylene [17].

Halogen molecules do not belong to any of these classes. On one hand, the long-range electron-molecule interaction is relatively weak, even in the case of interhalogen compounds. On the other hand, because the lowest anion state crosses the neutral curve very close to the equilibrium internuclear

separation, approximations involved in the local theory become invalid. In particular the local theory does not reproduce the correct threshold behavior of the DEA cross sections for F<sub>2</sub> and Cl<sub>2</sub> molecules, as discussed above.

It is therefore important to compare results of the nonlocal and local calculations performed with equivalent input parameters, the potential-energy curves and capture amplitudes. It is not clear what happens with regard to validity of the local theory when we turn to interhalogen molecules, like CIF. The inversion symmetry is broken in this case, and the *s*-wave contribution becomes essential. This is important for two reasons. First, the *s*-wave admixture changes the angular distribution of the products in the resonance scattering, particularly in the DEA process. Second, the widely used approximation for the capture amplitude *V* [18]

$$V = \left( \frac{\Gamma}{2\pi} \right)^{1/2}, \quad (1)$$

where  $\Gamma$  is the *total* resonance width, strictly speaking, is no longer valid, although it might be still reasonable for the calculation of the *total* (rather than angle-differential) cross section.

Whereas calculation of the total resonance width has become a standard procedure based on the Breit-Wigner parametrization of the eigenphase sums [19], calculation of the partial widths, resolved in angular momentum *l*, present a challenge. The partial width is defined within the framework of the Feshbach projection operator theory [20] or the resonance *R*-matrix theory [21]. *Ab initio* calculations using these theories are very challenging. Standard scattering codes generate the scattering matrix, and practically it would be more efficient to extract the partial width from scattering matrices, as it is usually done for the total width.

The purpose of this paper is twofold. First, we develop a method for calculation of partial widths based on the paper of Macek [22] and apply it to resonance *e*-CIF scattering. Our method is somewhat similar to that used by Haxton *et al.* [23] for calculation of angular distribution of the products in DEA to the water molecule, but is formulated in such a way that it

is easily extendable to the nonlocal treatment of the nuclear motion. Then we compare local and nonlocal versions of the DEA theory for the CIF molecule. The results turn out to be somewhat surprising, and we continue a similar investigation for electron attachment to  $F_2$ , the process relatively well studied in the past. We find that, in spite of the singular behavior exhibited by local cross sections at  $E \rightarrow 0$ , they produce thermal rate coefficients which are about a factor of 2 smaller than the nonlocal results.

## II. LOCAL THEORY

### A. $S$ matrix parametrization

According to the standard theory [24] the  $S$  matrix for resonance scattering can be represented as

$$S = S^0 - i \frac{\gamma \times \gamma}{E - E_R + i\Gamma/2}, \quad (2)$$

where  $S^0$  is the background  $S$  matrix,  $E$  is the projectile energy,  $E_R$  is the resonance energy,  $\Gamma$  is the total width,  $\gamma$  is the column of complex partial amplitudes  $\gamma_l$ , related to the partial capture amplitudes  $V_l$  as  $\gamma_l = \sqrt{2\pi} V_l$ ,  $l = 0, 1, \dots, l_{\max}$  where  $l_{\max}$  is the maximum number of partial waves included in calculations, and symbol  $\times$  indicates the direct product. The partial resonance width  $\Gamma_i$  is determined as

$$\Gamma_l = |\gamma_l|^2.$$

Because of the unitarity and time-reversal symmetry constraints we also have

$$S^0 \gamma^* = \gamma. \quad (3)$$

To incorporate this constraint automatically, we diagonalize first the background scattering matrix

$$e^{2i\delta^0} = U^T S^0 U,$$

where  $\delta^0$  is the diagonal matrix of background eigenphases, and  $U$  is a real orthogonal matrix diagonalizing  $S^0$  ( $T$  indicates the transposition). In practice it is obtained by diagonalization of the  $K^0$  matrix. Then  $\gamma$  can be written as [22]

$$\gamma = U e^{i\delta^0} x, \quad (4)$$

where  $x$  is a column of real numbers. This equation is equivalent to Eq. (3).

The parametrization procedure is reduced to the search for  $n(n+1)/2$  parameters defining the  $S^0$  matrix, where  $n = l_{\max} + 1$  is the number of channels, and  $n$  parameters defining the column  $x$  which satisfy the constraint

$$\sum_i x_i^2 = \Gamma.$$

In this local-theory version we neglect the energy dependencies of  $\gamma$  and  $S^0$  by choosing narrow enough energy interval.

### B. Results for CIF

The described procedure was applied to  $K$ -matrices calculated for  $e$ -CIF scattering for five internuclear separation  $R$  [25] with the use of the UCL  $R$ -matrix code [26–28]. The fitting interval was chosen with the center at the resonance position and the range about  $2\Gamma$ . Although five partial waves

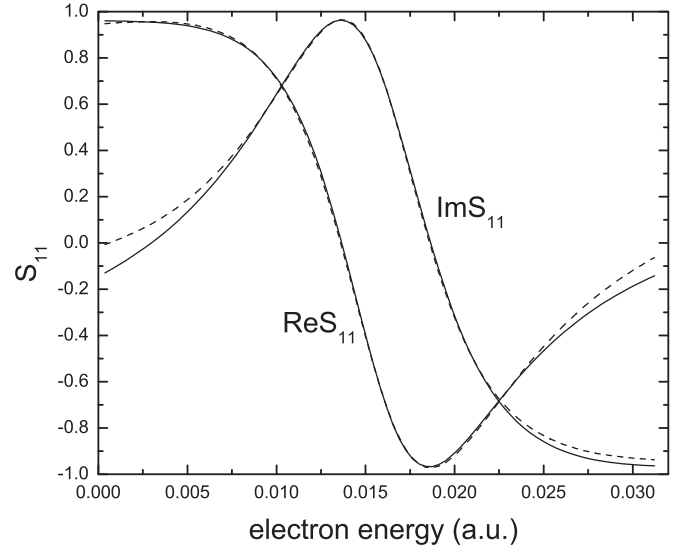


FIG. 1. Original (solid lines) and fitted (dashed lines) matrix element  $S_{11}$  for  $R = 2.9$  a.u.

( $l = 0$  through 4) have been included in calculations, only the first three give a noticeable contribution to the width. In Fig. 1 we present the fitting results for the matrix element  $S_{11}$  at  $R = 2.9$  a.u.

In Fig. 2 we present the first two parameters  $\gamma_l$ , and in Table I background phase shifts for  $l = 0, 1$ , and 2. Overall we see a decrease of  $|\gamma|$  with  $R$ , although a small instability at higher  $l$  appears. It is interesting that calculation of  $|\gamma|^2$  shows that the  $p$  wave dominates in the resonance scattering, although it is not apparent from the initial  $K$  matrices. This shows that, in spite of the broken inversion symmetry, resonance scattering in CIF is similar to  $Cl_2$  and  $F_2$ . However, at low energies the  $s$ -wave contribution becomes dominant, and this changes the threshold law for DEA [25].

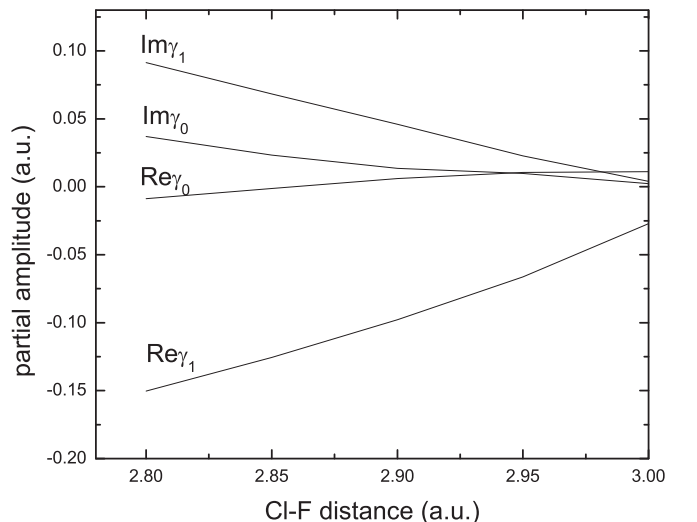


FIG. 2. Parameters  $\gamma_l$  for  $l = 0, 1$ .

TABLE I. Background eigenphases for  $e$ -CIF scattering.

$R$	$l = 0$	$l = 1$	$l = 2$
2.80	-0.6489	-0.3036	-0.010 08
2.85	-0.5774	-0.2475	-0.034 52
2.90	-0.5108	-0.1841	-0.040 82
2.95	-0.4588	-0.027 15	-0.027 10
3.00	-0.2595	-0.060 52	0.005 74

### C. Expansion of the capture amplitude in partial waves

For calculation of the DEA process, the capture amplitude should be expanded in partial waves and connected with the complex parameters  $\gamma_l$ . The exact phase factor in this relation is often ignored because of the approximate expression for the amplitude, Eq. (1). This relation, including the phase factor, was given in Ref. [23], but for the local version of the DEA theory. We present here some details applicable for the diatomic case which can be easily extended to the nonlocal version.

According to the Feshbach theory [20], the transition amplitude  $\mathcal{T}$  incorporating resonance scattering can be written as (the standard scattering amplitude is given by  $f = \mathcal{T}/k$ )

$$\mathcal{T} = \mathcal{T}_p + \frac{V_{\text{out}} V_{\text{in}}}{E - E_R + i\Gamma/2}, \quad (5)$$

where  $\mathcal{T}_p$  is the background transition amplitude, and the  $V_{\text{in}}$  and  $V_{\text{out}}$  amplitudes are

$$V_{\text{in}}(\mathbf{k}_i) = \langle \Phi \mathbf{V}_0^\dagger v^{(+)} \rangle, \quad V_{\text{out}}(\mathbf{k}_f) = \langle v^{(-)} \mathbf{V}_0 \Phi \rangle,$$

where  $\mathbf{V}_0$  is a unimatrix of coupling potentials,  $\Phi$  is a unimatrix representing the wave function of the resonance state,  $v^{(+)}$  is the initial wave function of the projectile with outgoing-wave boundary condition, and  $v^{(-)}$  is the final-state function corresponding to the ingoing wave boundary conditions.

In our case the partial-wave expansion of  $v^{(+)}$  has the form

$$v^{(+)} = \frac{2\pi i}{k} \sum_{l'} i^{l'} \frac{v_{l'}^m(r)}{r} Y_{l'm}^*(\hat{\mathbf{k}}) Y_{lm}(\hat{\mathbf{r}}), \quad (6)$$

where  $v_{l'}^m$  is a matrix (assume cylindrical symmetry for simplicity, so  $m$  is fixed) of radial wave functions which can be written as

$$\mathbf{v} = \mathbf{I} - \mathbf{O}\mathbf{S},$$

where  $\mathbf{I}$  and  $\mathbf{O}$  are matrices of ingoing-wave and outgoing-wave radial solutions.

Accordingly we can expand the “in” amplitude in partial waves as

$$V_{\text{in}}(\mathbf{k}_i) = \sum_l i^l \frac{\gamma_l}{\sqrt{2\pi}} Y_{lm}^*(\hat{\mathbf{k}}_i). \quad (7)$$

Using the relation between the ingoing wave and outgoing wave solutions [29], we also obtain

$$V_{\text{out}}(\mathbf{k}_f) = \sum_l i^{-l} \frac{\gamma_l}{\sqrt{2\pi}} Y_{lm}(\hat{\mathbf{k}}_f). \quad (8)$$

Expansion (7) is written in the body frame with the polar axis along the internuclear axis. It can be rewritten in terms

of the angular coordinates  $\hat{\mathbf{R}}$  characterizing direction of the molecular axis with respect to the direction of the momentum  $\mathbf{k}$  [30]

$$V_{\text{in}}(\mathbf{k}_i) = (-1)^m \sum_l i^l \frac{\gamma_l}{\sqrt{2\pi}} Y_{lm}^*(\hat{\mathbf{R}}).$$

Parameters  $\gamma_l$  can be determined from the appropriately normalized solution (6). However, this is unnecessary for our purposes since it can be proven that they are identical to those entering Eq. (2). Expand first the transition amplitude in partial waves [31]

$$\mathcal{T} = 2\pi i \sum_{ll'm} i^{l'-l} T_{ll'} Y_{l'm}^*(\mathbf{k}_i) Y_{lm}(\mathbf{k}_f),$$

where  $T_{ll'}$  is the transition matrix in the angular-momentum representation. (We use the definition  $T = 1 - S$ .) Comparing this expansion with Eqs. (5), (7), and (8), we find

$$T_{ll'}^{res} = i \frac{\gamma_l \gamma_{l'}}{E - E_R + i\Gamma/2}$$

that is consistent with Eq. (2).

For DEA calculations only the entrance projectile amplitude is necessary. According to the general theory [32], the wave function  $\psi_v(\mathbf{r})$  of the outgoing fragments can be written as

$$\psi_v(\mathbf{r}) = \sum_l \frac{\xi_{vl}(R)}{R} Y_{lm}(\hat{\mathbf{R}}),$$

where subscript  $v$  indicates the initial vibrational state. The radial function  $\xi_{vl}(R)$  satisfies the equation

$$\begin{aligned} & \left( -\frac{1}{2M} \frac{d^2}{dR^2} + U(R) - i\Gamma(R)/2 - E \right) \xi_{vl}(R) \\ & = -i^l \frac{\gamma_l(R)}{\sqrt{2\pi}} \zeta_v(R), \end{aligned} \quad (9)$$

where  $U(R)$  is the potential-energy function for the anion, and  $\zeta_v(R)$  is the vibrational wave function for the initial state. Equation (9) assumes the axial recoil approximation [30] which works well for diatomic molecules if the collision time is short compared to the rotational period. The solution of this equation, satisfying the outgoing-wave boundary condition, is

$$\xi_{vl}(R) = -i^l \int G(R, R') \frac{\gamma_l(R')}{\sqrt{2\pi}} \zeta_v(R') dR', \quad (10)$$

where  $G(R, R')$  is the Green's function of the left-hand side of Eq. (9) corresponding to the outgoing-wave boundary condition. The differential cross section is given by

$$\frac{d\sigma}{d\Omega} = \frac{2\pi^2 K}{k^2 M} \lim_{R \rightarrow \infty} \left| \sum_l \xi_l(R) Y_{lm}(\hat{\mathbf{R}}) \right|^2. \quad (11)$$

This expression can be simplified using the Franck-Condon (FC) principle. Equation (10) can be rewritten as [33]

$$\xi_{vl}(R) = -i^l \frac{\gamma_l(R_v)}{\sqrt{2\pi}} \int G(R, R') \zeta_v(R') dR', \quad (12)$$

where the FC point  $R_v$  is determined from the equation

$$E - W(R_v) = \epsilon_v - V_0(R_v), \quad (13)$$

where  $V_0(R)$  is the potential-energy curve for the neutral molecule,  $W(R) = U(R) - i\Gamma(R)/2$  is the complex potential entering Eq. (9), and  $\epsilon_v$  is the energy of the initial vibrational state. In this approximation the  $l$  dependence of the DEA amplitude is given by  $\gamma_l(R_v)$ ; therefore, the differential cross section is given by the expression

$$\frac{d\sigma}{d\Omega} = a_v \left| \sum_l i^l \gamma_l(R_v) Y_{lm}^*(\hat{\mathbf{R}}) \right|^2, \quad (14)$$

where the  $l$ -independent parameter  $a_v$  can be expressed in terms of the total cross section  $\sigma_v$  as

$$a_v = \frac{\sigma_v}{\Gamma(R_v)}.$$

Note that according to Eq. (13) the FC point is complex. This requires an analytical continuation of the amplitudes  $\gamma_l(R)$  into the complex  $R$  plane. However, our  $\gamma_l(R)$  is not determined accurately enough for this purpose. Assuming that the resonance is narrow enough, we can solve Eq. (13) with  $\text{Re}W(R) = U(R)$ . For wide resonances the local theory fails anyway.

#### D. Results for cross sections

The results for the integrated DEA cross sections calculated according to Eqs. (9) do not differ substantially from those obtained in Ref. [25] based on the approximation for the capture amplitude, Eq. (1). This is demonstrated in Fig. 3. The two curves become distinguishable only above  $E = 0.5$  eV where the cross section is relatively small. This difference does not affect the thermal rate coefficients calculated in Ref. [25].

It is known, though, that the local theory violates the Wigner threshold law behavior at low energies. Sometimes this deficiency is corrected by multiplying the attachment

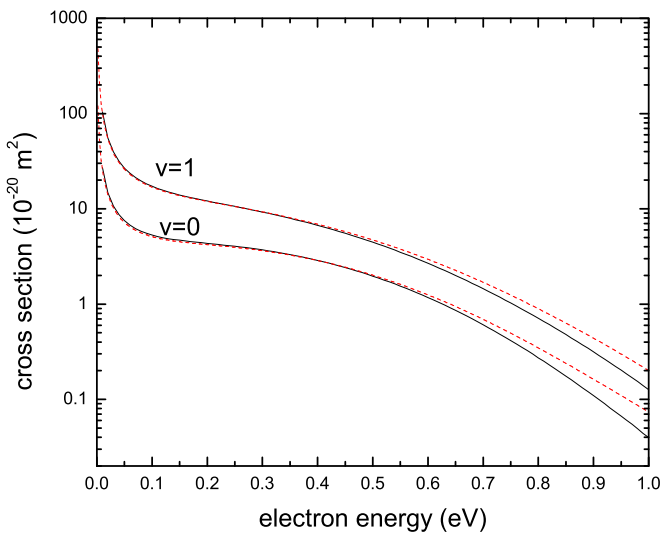


FIG. 3. Local calculations of DEA cross sections for CIF in the ground and first excited vibrational states. Solid (black) curves: with approximation (1). Dashed (red) curves: without approximation (1). Bardsley correction is not included.

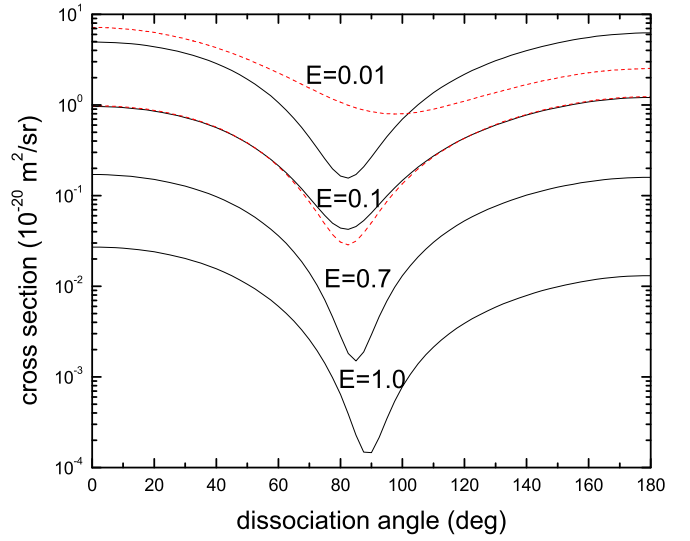


FIG. 4. Differential DEA cross sections for selected energies indicated in eV. At  $E = 0.01$  and  $0.1$  eV the cross sections calculated with the use of the FC approximation are also shown by dashed (red) curves.

amplitude by a factor introduced by Bardsley [34]

$$c = (E/E_r(R))^{a/2}, \quad (15)$$

where  $E_r(R) = U(R) - V_0(R)$  is the resonance energy at a given  $R$  and  $a$  is the threshold exponent. For nonpolar molecules, according to the Wigner law  $a = l_{\min} + 1/2$ . For the  $l$ -dependent amplitude the correction factor should become  $l$  dependent as well, and the threshold exponent becomes  $a_l = l + 1/2$ . It is known, however, that the Bardsley correction can underestimate DEA cross sections that were indeed observed in Ref. [25]. Moreover, our calculations have shown that the choice  $a_l = l + 1/2$  produces cross sections which are substantially smaller than those calculated in Ref. [25]; therefore, the  $E^{1/2}$  scaling seems to be more reasonable. While the complete answer to the question about the correction factor requires nonlocal calculations, it is safe to conclude at this point that the present calculations of the integrated cross sections confirm the results of Ref. [25].

In Fig. 4 we present differential cross sections for selected energies. We also check the validity of the FC approximation by presenting the results of local calculations obtained by direct calculation of the integral (10) and by the use of the FC approximation, Eq. (12). The FC approximation works very well except at low energies below  $0.1$  eV. In this region the nuclear motion is very slow and the FC principle is less valid. However, the FC approximation affects very little the integrated cross sections even in the low-energy region. These observations are important for interpretation of nonlocal results discussed below.

It is apparent that the  $l = 1$  component is dominant even at relatively low energies, although theoretically with decreasing energies the  $s$ -wave component should take over. The local theory without the Bardsley correction is not able to describe this transition. In order to do this within the local formalism we have to introduce the  $l$ -dependent coefficient, Eq. (15), with  $a_l = l + 1/2$ . However, this modification

strongly reduces the total cross section and seems to be inadequate.

### III. NONLOCAL THEORY

#### A. Basic formalism

Nonlocal theory requires calculation of the width function  $\Gamma(R, E)$  depending both on the internuclear separation and electron energy. Whereas calculation of the local width for a sufficiently narrow resonance is straightforward, the nonlocal width contains more information than the on-shell scattering matrix. This can be seen from the expression for the Feshbach width

$$\Gamma(E) = 2\pi |\langle \Phi \mathbf{V}_0^\dagger v_E^{(+)} \rangle|^2,$$

which involves the scattering wave function  $v_E^{(+)}$  rather than the scattering matrix.

A completely *ab initio* calculation of  $\Gamma(R, E)$  is a very challenging task even for simple diatomics and was done only in a few cases. It is more customary in practice to parametrize the width as a function of  $E$  and fit the parameters to reproduce *ab initio* scattering matrices [10]. Although this procedure is somewhat ambiguous, it usually gives a satisfactory way to include the nonlocal effects in the DEA theory. The function  $\Gamma(E)$  for a given  $R$  should have a proper threshold behavior and decay at  $E \rightarrow \infty$ . A simple formula satisfying these requirements is [10]

$$\Gamma(E) = Ax^a e^{-x}, \quad x = E/B, \quad (16)$$

where  $A$  and  $B$  are fit parameters and  $a$  is the threshold exponent. In the absence of the dipolar interaction  $a = l_{\min} + 1/2$  where  $l_{\min}$  is the lowest electron angular momentum allowed by symmetry.

The corresponding parametrization of the parameters  $\gamma_l(E)$  can be chosen as

$$\gamma_l(E) = g_l e^{-x/2} x^{a_l/2}. \quad (17)$$

Because of the small value of the dipole moment of the CIF molecule we have chosen

$$a_l = l + 1/2.$$

This approximation is reasonable, since inclusion of nonzero value of the dipole moment in the local calculations produced negligible changes in the cross sections. To reduce the ambiguity in fitting, we have also assumed that  $l$  dependence of the parameter  $g_l$  is the same as in the local theory; therefore,

$$g_l = s\gamma_l^{\text{local}}, \quad (18)$$

where  $s$  is an  $l$ -independent parameter. Therefore, the fitting at each value of the internuclear distance  $R$  is reduced to determination of  $s$  and  $B$ . The resulting fit parameters are presented in Table II.

To increase somewhat flexibility of the fit procedure, we have also introduced  $l$ -dependent parameter  $B$ . As will be shown below, the results for the DEA cross sections, obtained from the two sets of corresponding parameters, do not differ significantly.

In Fig. 5 we present the results for  $\Gamma(E)$  obtained from the fit for several internuclear separations.

TABLE II. CIF: parameters for the nonlocal width entering Eqs. (16)–(18) in a.u.

$R$	$B$	$s$
2.80	0.017 115	1.2909
2.85	0.012 883	1.3253
2.90	0.008 412	1.4142
2.95	0.004 810 6	1.4487
3.00	0.001 738	1.5744

The capture amplitude of the nonlocal theory is given by Eq. (7) with the only difference that the parameter  $\gamma_l$  is now energy dependent. The partial wave function describing the motion of outgoing fragments is given by the equation similar to Eq. (9)

$$\left( -\frac{1}{2M} \frac{d^2}{dR^2} + U(R) + F - E \right) \xi_l(R) = -i^l \frac{\gamma_l(R)}{\sqrt{2\pi}} \zeta_v(R). \quad (19)$$

The major difference with the local theory is that it contains a nonlocal energy-dependent operator  $F$  whose explicit expression was given by Bardsley [32] and, in more detail, by Domcke [10]. Kalin and Kazansky [35] worked out a quasiclassical representation for this operator, based on the FC principle, which simplifies the solution of the nonlocal problem. The same method is used in the present paper.

The FC principle can be also used for evaluation of the angular distribution of the products. The result is given by the same Eq. (14) of the local theory, except that  $\gamma_l(E, R_v)$  are now nonlocal energy-dependent amplitudes with the correct threshold behavior. Note that in the nonlocal theory we are dealing with the real diabatic anion curve  $U(R)$ ; therefore, the FC point is always real, and no additional approximations in solving Eq. (13) are involved.

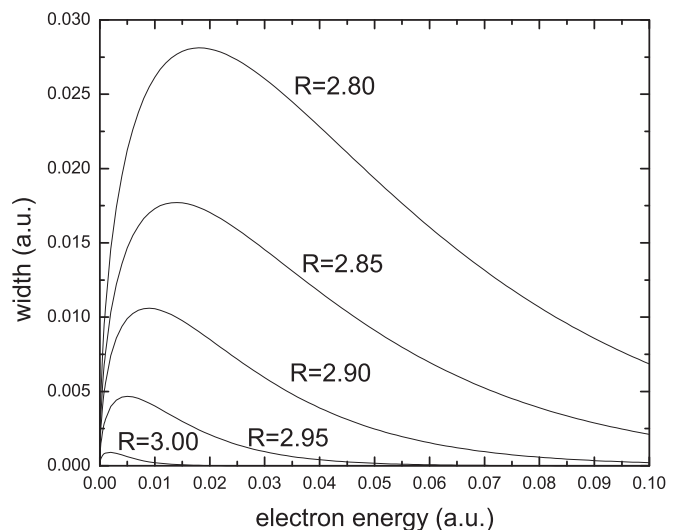


FIG. 5. Width for CIF plotted as a function of energy  $E$  for several internuclear distances indicated in a.u.

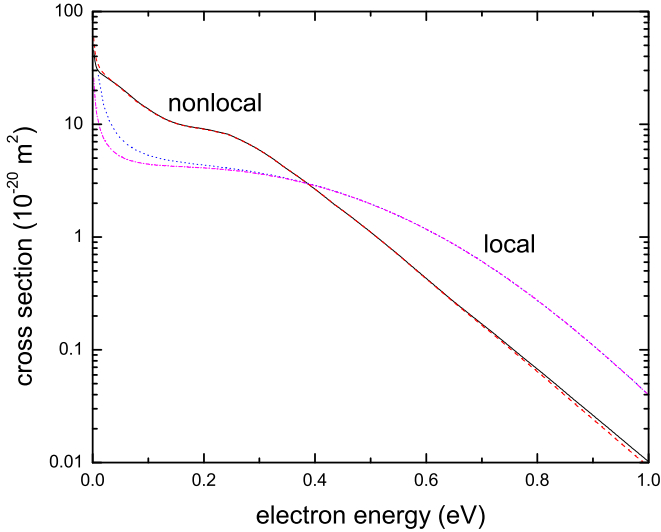


FIG. 6. DEA cross sections for CIF in the ground vibrational state. Nonlocal calculations: solid (black) curve, with  $l$ -dependent parameter  $B$ ; dashed (red) curve, with  $l$ -independent parameter  $B$ . Local calculations: dotted (blue) curve, without Bardsley correction; dot-dashed (magenta) curve, with Bardsley correction.

### B. Comparison of nonlocal and local theories

In Fig. 6 we present comparison of four sets of the cross sections: results of local calculations without Bardsley correction, local calculations with the Bardsley correction, and the nonlocal calculations with  $l$ -independent and  $l$ -dependent parameter  $B$  in Eq. (16). The last two results are almost indistinguishable. However, the local results, even without the Bardsley correction, lie below the nonlocal calculations at low energies. Only below 0.01 eV, due to the  $1/E$  behavior, they exceed the nonlocal results. The cross section calculated with Bardsley correction exhibit the correct threshold behavior, but lie well below the nonlocal results. On the other hand, at higher electron energies ( $E > 0.4$  eV) the local results become higher than nonlocal.

In Fig. 7 we present angular distributions. As expected, the nonlocal theory shows the transition from the  $p$ -wave dominated differential cross section to the  $s$ -wave dominated. However, the transition occurs at a very low energy region about 0.01 eV. Therefore, DEA to interhalogens, in our case to the CIF molecule, preserves the properties of DEA to homonuclear halogens down to low energies. We should also note that our nonlocal results are obtained with the use of the FC principle; therefore, quantitatively they become less accurate at lower energies, although the transition from the  $p$ -wave dominance to the  $s$ -wave dominance is described qualitatively correctly. These results might be interesting in connection with recent observation of unexpected angular distribution in DEA to  $\text{Cl}_2$  [36].

### C. Nonlocal theory: Comparison with $\text{F}_2$

Comparison of local with nonlocal results for the total DEA cross sections for CIF looks surprising. It is even somewhat disappointing because the nonlocal cross sections generate thermal rate coefficients which are about a factor of 2 higher

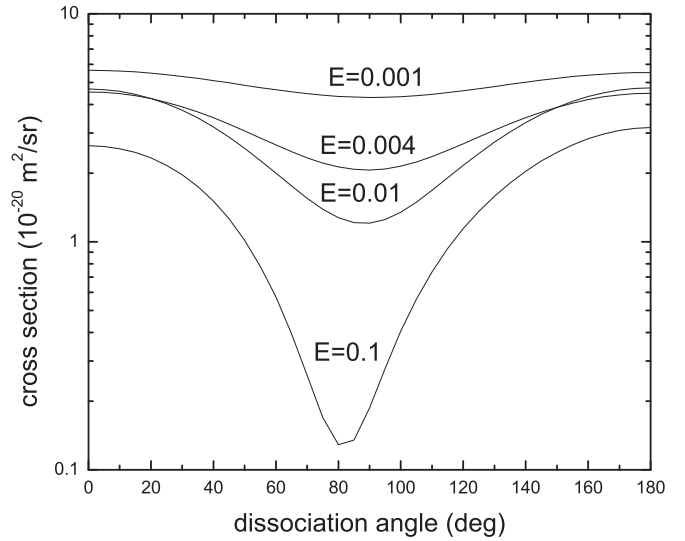


FIG. 7. Differential DEA cross sections for CIF in its ground vibrational state for selected energies calculated by the nonlocal theory.

than those obtained from the local calculations [25], and the latter agree quite well with the flowing afterglow-Langmuir probe (FALP) experiment [25]. On the other hand, our previous nonlocal calculations of rate coefficients for  $\text{Cl}_2$  [8] and  $\text{F}_2$  [9] also agree very well with FALP measurements.

To investigate the problem further, we performed local and nonlocal calculations of DEA to  $\text{F}_2$  through the  $\Sigma_u$  resonance using potential curves and fixed-nuclei  $K$  matrices [37] calculated by the same *ab initio* methods as in Ref. [25]. Since the DEA process at low energies is dominated by the  $p$  wave in this case, we included only two terms,  $l = 1$  and 3 in the partial-wave expansion, and did not analyze the angular distribution. The total nonlocal width was parametrized according to Eq. (16) with the threshold exponent  $a = 3/2$ . In Table III we present the fit parameters  $A$ ,  $B$ , and the total local width  $\Gamma^{\text{loc}}$  for six internuclear separations. As in the case of CIF, the parameters were obtained from the fit to the *ab initio*  $K$  matrices [37].

The results for DEA cross sections are presented in Fig. 8, where we also compare with previous resonance  $R$ -matrix calculations [9] in which the  $R$ -matrix parameters were fixed by adjusting the resonance width to the results of Hazi *et al.* [38]. The resonance  $R$ -matrix theory is completely equivalent to the nonlocal theory [39]; therefore, the difference between the results of two calculations should be attributed

TABLE III.  $\text{F}_2$ : parameters for the nonlocal width entering Eq. (16), and the local width  $\Gamma^{\text{loc}}$ ; all quantities are in a.u.

$R$	$B$	$A$	$\Gamma^{\text{loc}}$
2.40	0.048 82	0.1790	0.065 64
2.45	0.044 34	0.1553	0.049 27
2.50	0.037 37	0.1236	0.033 53
2.55	0.029 13	0.0884	0.019 82
2.60	0.019 57	0.0507	0.009 06
2.65	0.008 05	0.0141	0.001 89

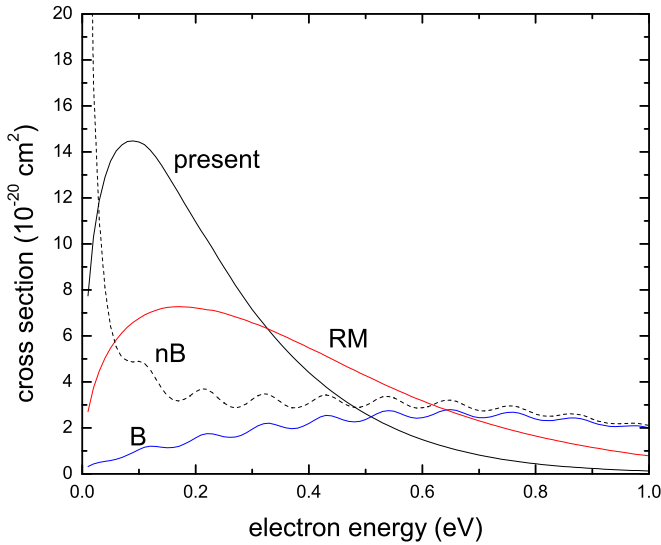


FIG. 8. DEA cross sections for the  $F_2$  molecule in the ground vibrational state. Solid (black) line: present nonlocal theory; solid (red) line RM: resonance  $R$ -matrix calculations [9] with the resonance width adjusted to Hazi *et al* [38]; dashed (black) line nB and solid (blue) line B: local theory without and with Bardsley correction, respectively.

to different resonance width. On the other hand, the local cross sections are very different from both calculations. At  $E < 0.4$  eV the local theory results are substantially lower than nonlocal, except the low-energy region below 0.03 eV where the calculations without Bardsley correction exhibit the  $1/E$  divergence. Similar results for DEA to the  $F_2$  molecule were obtained by Houfek *et al.* [40]: their local cross sections for the “ $F_2$ -like model” are substantially smaller than nonlocal in the energy interval between 0.03 and 0.6 eV. It is also interesting that the exact cross sections obtained within the framework of their model are close to the results of the nonlocal theory whose only assumption is the Born-Oppenheimer approximation.

In addition, our local theory results exhibit an oscillatory structure. These oscillations are not unexpected, and might appear [41] due to the oscillatory energy dependence of the survival factor defined as [42]

$$s = |S|, \quad (20)$$

where  $S$  is the nonunitary scattering matrix obtained from the solution of Eq. (9) with the zero right-hand side. To understand better the structure of the local cross section it is useful to analyze it from the point of view of the quasiclassical (WKB) theory. The quasiclassical approximation leads to the representation of the DEA cross section as a product of the capture cross section and the survival factor. However, expressions for these quantities depend on a specific version of the WKB expansion. In the original theories of Bardsley, Herzenberg, and Mandl [43] and O’Malley [42] the expansion of the WKB wave function is carried out about the classical turning point for the anion motion. A more rigorous quasiclassical theory is based on the saddle-point technique with the uniform Airy function approximation [33]. Application of this method leads to the FC transition point  $R_v$  defined by Eq. (13). Although the FC point is complex, we will neglect again its imaginary

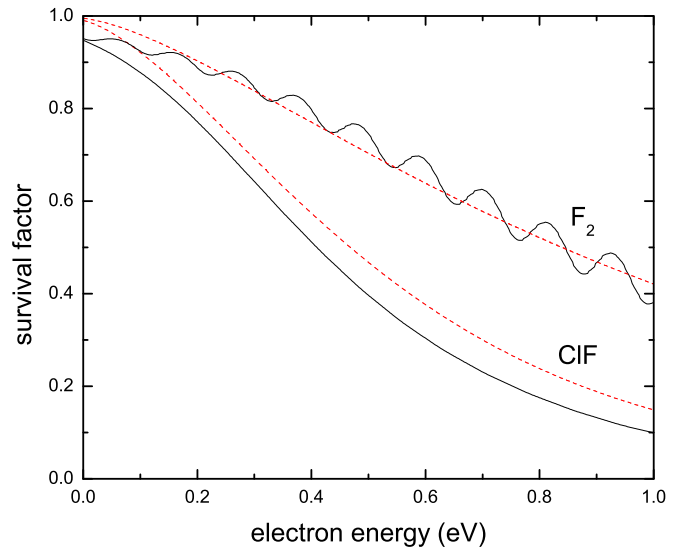


FIG. 9. Survival factor of the local theory for  $F_2$  and ClF. Solid (black) curves: exact result from Eq. (20). Dashed (red) curves: WKB approximation, Eq. (22).

part that introduces a small error for narrow resonances. This approximation is traditional in WKB versions of the local theory [42,43]. The result for the DEA cross section in this approximation can be written as

$$\sigma = \frac{\pi^2}{E} \Gamma(R_v) F_v(E) s, \quad (21)$$

where  $F_v(E)$  is the generalized FC factor for which a uniform Airy function approximation has been worked out by Kazansky and Yelets [33]. The survival factor in the WKB approximation is well known [32,43]. Assuming also a small resonance width, we can simplify it further as

$$s = \exp\left(-\int_{a_-}^{R_s} \frac{\Gamma(R)}{v(R)} dR\right), \quad (22)$$

where  $v(R)$  is the classical velocity for the anion motion and  $a_-$  is the turning point for the anion motion. We neglect again the imaginary part of  $a_-$ .

In Fig. 9 we compare the exact survival factor, Eq. (20), with the approximate survival factor calculated from Eq. (22). It is apparent that the oscillations in the exact survival factor lead to the oscillations in the DEA cross sections. It is interesting, though, that for heavier targets these oscillations disappear. In the same figure we show comparison of survival factors for ClF. No oscillations are seen in the exact survival factor for ClF. At zero electron energy the approximate survival factor is equal to 1, although the exact survival factor is somewhat smaller due to contribution of internuclear distances left of the transition point.

In Fig. 10 we compare the WKB version of the local theory with nonlocal calculations. Although both versions of the local theory are substantially different from the nonlocal results, in the low-energy region the WKB version produces much better results than the exact local theory. As can be seen from Eq. (21), the threshold behavior is determined by the ratio  $\Gamma(R_v)/E$ . When  $E \rightarrow 0$  the FC point  $R_v$  approaches the

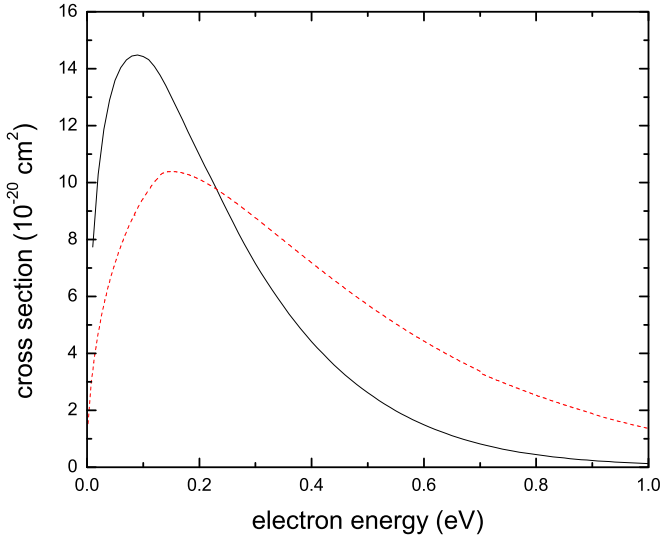


FIG. 10. DEA cross section for  $F_2$ , comparison of the present nonlocal results, solid (black) curve, with the WKB version of the local theory, dashed (red) curve.

crossing (stabilization) point  $R_s$ ; therefore, if for  $R \rightarrow R_s$  the width  $\Gamma$  is parametrized as

$$\Gamma(R) = \text{const} \times (U(R) - V_0(R))^a,$$

then according to Eq. (13)

$$\Gamma(R_v) = \text{const} \times E^a,$$

where  $a$  is the correct threshold exponent ( $3/2$  in case of  $F_2$ ), and the cross section exhibits the correct low-energy behavior as shown in Fig. 10.

We conclude that the WKB version of the local theory works better than the exact local theory itself. A similar conclusion can be drawn from comparison of the two versions of the local theory for CIF. Although a complete analysis of this interesting phenomenon is beyond the scope of the present paper, we present here two important points.

(1) Since there is one-to-one correspondence between the electron energy and the transition point in the WKB version, it is easier to enforce the correct threshold behavior in the WKB version as discussed above, whereas the Bardsley correction of the exact local theory might strongly underestimate the DEA cross section.

(2) In both theories involving the WKB approximation (local and nonlocal) we also use the FC approximation. It might be argued that this can cause a similarity between our nonlocal calculation and the WKB version of the local theory, just reflecting the error of the WKB and FC approximations. However, the fact that our previous  $R$ -matrix calculations for  $F_2$  [9], based on the WKB approximation, agree with the quantum-mechanical calculations of Hazi *et al.* [38], indicates that the WKB approximation and FC principle work very well in this system.

This brings us back to the point of comparison between the local theory, nonlocal theory, and experiment. As can be seen from Fig. 8, our previous calculations for  $F_2$ , based on the data of Hazi *et al.* [38] for the resonance width, in the low-energy region are about a factor of 2 lower than the present

calculations. The analysis of the corresponding resonance width leads to the same conclusion: the present resonance width is about a factor of 2 higher than one calculated in Ref. [38]. Since at low electron energies the survival factor is close to 1, the cross section is roughly proportional to the resonance width at the FC point, and this explains the factor of 2 difference between the present cross sections at low energies and those calculated in Ref. [9]. The same argument can be presented for the thermal rate coefficient.

This is helpful for analysis of our results for CIF. A reason for disagreement of the thermal rate coefficients calculated from the nonlocal cross section with experimental rate coefficients might be an overestimation of the width by a factor of 2 in the region of internuclear distances close to the crossing point. On the other hand, the local theory, for a given width, underestimates the thermal rate coefficients. Therefore, our local results [25] agree well with experiments. It should be stressed, however, that due to the sensitivity of the DEA cross sections to all aspects of the theory, including the method of calculation of fixed-nuclei parameters and the nuclear dynamics, the factor of 2 accuracy should be considered as good. We also stress that at low energies the DEA cross section is extremely sensitive to the behavior of the width near the crossing point. Additional nonlocal calculations for CIF have shown that the thermal rate coefficient can be easily reduced by a factor of 2 by reducing the width only at  $R \geq 3$  a.u. (with the crossing point  $R_s = 3.02$ ). This is the range of internuclear distances where the accurate calculation of the resonance width is particularly very challenging. As was shown in Ref. [44], different methods of calculation of the resonance width for  $F_2$  give very different results which sometimes differ by the order of magnitude. (We should note, though, that the results of Hazi *et al.* [38] for the width are plotted in Ref. [44] incorrectly). Because of such difficulties in accurate calculation of  $\Gamma(R)$ , DEA experiments can actually serve as a method of calibration of this function. In the case of  $F_2$  it appears that the 35-year-old results of Hazi *et al.* for the width are the most accurate for the purpose of calculation of thermal DEA rate coefficients as demonstrated in Ref. [9].

#### IV. CONCLUSION

The presented results confirm once again that calculation of DEA cross section is a very nontrivial task, even if all fixed-nuclei input parameters are known. Although the local version of the DEA theory turned out to be successful for several nonpolar molecules, the halogen molecules represent another example, in addition to hydrogen halides, where nonlocal calculations are necessary for an accurate description of cross sections and thermal rate coefficients. This is mainly due to a special behavior of the neutral and anion curves in the Franck-Condon region: they cross very close to the equilibrium internuclear separation for the neutral. Whereas at very low energies the local theory overestimates DEA cross sections due to the  $1/E$  divergence, at higher-energy region, important for calculation of thermal rate coefficients, the local results are lower than nonlocal. Investigation of the quasiclassical version of the local theory is helpful in understanding the difference between the local and nonlocal results.

Our results for differential cross sections for DEA to CIF show the dominance of the  $p$ -wave contribution to

the DEA process above  $E = 0.01$  eV. Below this energy a graduate transition from the  $p$ -wave dominance to the  $s$ -wave dominance occur. This tells us that in spite of the inversion symmetry breaking in CIF, the DEA process in this interhalogen molecule is similar to that in homonuclear halogens  $F_2$  and  $Cl_2$ .

### ACKNOWLEDGMENTS

The author thanks V. Kokoouline for providing his unpublished results for  $e-F_2$  fixed-nuclei scattering matrices. This work was supported by the US National Science Foundation under Grant No. PHY-1401788.

- 
- [1] W.-C. Tam and S. F. Wong, *J. Chem. Phys.* **68**, 5626 (1978).  
 [2] L. G. Christophorou and J. K. Olthoff, *J. Phys. Chem. Ref. Data* **28**, 131 (1999).  
 [3] E. P. Wigner, *Phys. Rev.* **73**, 1002 (1948).  
 [4] D. Klar, M.-W. Ruf, and H. Hotop, *Chem. Phys. Lett.* **189**, 448 (1992); *Aust. J. Phys.* **45**, 263 (1992).  
 [5] S. Barsotti, M.-W. Ruf, and H. Hotop, *Phys. Rev. Lett.* **89**, 083201 (2002).  
 [6] M.-W. Ruf, S. Barsotti, M. Braun, H. Hotop, and I. I. Fabrikant, *J. Phys. B* **37**, 41 (2004).  
 [7] M. Braun, M.-W. Ruf, I. I. Fabrikant, and H. Hotop, *Phys. Rev. Lett.* **99**, 253202 (2007).  
 [8] J. F. Friedman, T. M. Miller, L. C. Schaffer, A. A. Viggiano, and I. I. Fabrikant, *Phys. Rev. A* **79**, 032707 (2009).  
 [9] N. S. Shuman, T. M. Miller, A. A. Viggiano, and I. I. Fabrikant, *Phys. Rev. A* **88**, 062708 (2013).  
 [10] W. Domcke, *Phys. Rep.* **208**, 97 (1991).  
 [11] I. I. Fabrikant, *Phys. Rev. A* **43**, 3478 (1991).  
 [12] C. Mündel, M. Berman, and W. Domcke, *Phys. Rev. A* **32**, 181 (1985).  
 [13] M. Čížek, J. Horáček, and W. Domcke, *Phys. Rev. A* **60**, 2873 (1999).  
 [14] M. Čížek, J. Horáček, A.-Ch. Sergenton, D. B. Popović, M. Allan, W. Domcke, T. Leininger, and F. X. Gadea, *Phys. Rev. A* **63**, 062710 (2001).  
 [15] M. Čížek, J. Horáček, M. Allan, I. I. Fabrikant, and W. Domcke, *J. Phys. B* **36**, 2837 (2003).  
 [16] I. I. Fabrikant, *J. Phys. Conf. Ser.* **192**, 012002 (2009).  
 [17] S. T. Chourou and A. E. Orel, *Phys. Rev. A* **77**, 042709 (2008).  
 [18] D. T. Birtwistle and A. Herzenberg, *J. Phys. B* **4**, 53 (1971).  
 [19] A. U. Hazi, *Phys. Rev. A* **19**, 920 (1979).  
 [20] H. Feshbach, *Ann. Phys. (N.Y.)* **5**, 357 (1958).  
 [21] A. M. Lane and R. G. Thomas, *Rev. Mod. Phys.* **30**, 257 (1958).  
 [22] J. Macek, *Phys. Rev. A* **2**, 1101 (1970).  
 [23] D. J. Haxton, C. W. McCurdy, and T. N. Rescigno, *Phys. Rev. A* **73**, 062724 (2006).  
 [24] J. R. Taylor, *The Quantum Theory of Nonrelativistic Collisions* (Dover, Mineola, NY, 2000).  
 [25] J. P. Wiens, J. C. Sawyer, T. M. Miller, N. S. Shuman, A. A. Viggiano, M. Khamesian, V. Kokoouline, and I. I. Fabrikant, *Phys. Rev. A* **93**, 032706 (2016).  
 [26] J. Tennyson, D. B. Brown, J. J. Munro, I. Rozum, H. N. Varambhia, and N. Vinci, *J. Phys. Conf. Ser.* **86**, 012001 (2007).  
 [27] J. Tennyson, *Phys. Rep.* **491**, 29 (2010).  
 [28] J. M. Carr, P. G. Galiatsatos, J. D. Gorfinkiel, A. G. Harvey, M. A. Lysaght, D. Madden, Z. Mašín, M. Plummer, J. Tennyson, and H. N. Varambhia, *Eur. Phys. J. D* **66**, 58 (2012).  
 [29] L. D. Landau and E. M. Lifshitz, *Quantum Mechanics (Non-relativistic theory)* (Pergamon Press, New York, 1965).  
 [30] T. F. O'Malley and H. S. Taylor, *Phys. Rev.* **176**, 207 (1968).  
 [31] N. F. Lane, *Rev. Mod. Phys.* **52**, 29 (1980).  
 [32] J. N. Bardsley, *J. Phys. B* **1**, 349 (1968).  
 [33] A. K. Kazansky and I. S. Yelets, *J. Phys. B* **17**, 4767 (1984).  
 [34] J. N. Bardsley, in *Electron-Molecule and Photon-Molecule Collisions*, edited by T. Rescigno, V. McKoy, and B. Schneider (Plenum, New York, 1979).  
 [35] S. A. Kalin and A. K. Kazansky, *J. Phys. B* **23**, 4377 (1990).  
 [36] K. Gope, V. S. Prabhudesai, N. J. Mason, and E. Krishnakumar, *J. Phys. B* **49**, 015201 (2016).  
 [37] V. Kokoouline (unpublished).  
 [38] A. U. Hazi, A. E. Orel, and T. N. Rescigno, *Phys. Rev. Lett.* **46**, 918 (1981).  
 [39] I. I. Fabrikant, *Comments At. Mol. Phys.* **24**, 37 (1990).  
 [40] K. Houfek, T. N. Rescigno, and C. W. McCurdy, *Phys. Rev. A* **77**, 012710 (2008).  
 [41] G. A. Gallup, *J. Chem. Phys.* **126**, 064101 (2007).  
 [42] T. F. O'Malley, *Phys. Rev.* **150**, 14 (1966).  
 [43] J. N. Bardsley, A. Herzenberg, and F. Mandl, *Proc. R. Soc.* **89**, 321 (1966).  
 [44] M. Honigmann, R. J. Buenker, and H. P. Liebermann, *J. Comput. Chem.* **33**, 355 (2012).